Water vapor transport in the vicinity of imbibing saline plumes: Homogeneous and layered unsaturated porous media

Noam Weisbrod

Department of Environmental Hydrology and Microbiology, Institute for Water Sciences and Technologies, Desert Research Institutes, Ben-Gurion University of the Negev, Sede-Boqer Campus, Israel

Michael R. Niemet,[1] Thomas McGinnis, and John S. Selker

Department of Bioengineering, Oregon State University, Corvallis, Oregon, USA

Received 24 June 2002; revised 17 October 2002; accepted 13 March 2003; published 6 June 2003.

[1] Water vapor transport in the vicinity of imbibing saline solutions was investigated in two-dimensional (2-D) chambers using a light transmission technique. Concentrated $NaNO_3$ solutions (brines) were applied as point sources to the surface of homogenous packs of prewetted silica sand for four different sand grades. The same solutions were applied to layered systems, where two horizontal fine layers were embedded within a coarser matrix, mimicking stratified sedimentary deposits. Water vapor transport from the residually saturated sand into the imbibing brine was observed in all sand grades and geometries. Pure water applied to sand prewetted with brine migrated into the surrounding residual brine. Water vapor stripping was found to enhance the lateral transport of brine in layered sand, where capillary barrier effects play a major role. Our observations suggest that osmotic potential and vapor density lowering in saline solutions, often neglected in predictive models, should be taken into account when predicting the transport of brines in the vadose zone. *INDEX TERMS:* 1829 Hydrology: Groundwater hydrology; 1831 Hydrology: Groundwater quality; 1832 Hydrology: Groundwater transport; 1866 Hydrology: Soil moisture; 1875 Hydrology: Unsaturated zone; *KEYWORDS:* vapor transport, osmotic potential, unsaturated zone, saline solution, brine, layered porous media

Citation: Weisbrod, N., M. R. Niemet, T. McGinnis, and J. S. Selker, Water vapor transport in the vicinity of imbibing saline plumes: Homogeneous and layered unsaturated porous media, *Water Resour. Res.*, *39*(6), 1145, doi:10.1029/2002WR001539, 2003.

1. Introduction

[2] In most natural settings the salt concentration of the pore water is relatively low and thus the vapor density depression is negligible. Under landfills, waste facilities, and industrial complexes, hypersaline solutions (brines) may infiltrate from the land surface into the underlying vadose zone. For example, at the Hanford site in southeast Washington State, large amounts of highly radioactive brines (>5 mol/l Na) have leaked from storage tanks into the surrounding vadose zone over the last 50 years [*Grand Junction Projects Office* (*GJPO*), 1996]. In this case, it is possible that a depression in vapor density at the periphery of the infiltrating brine has resulted in water vapor transport from the native soil into the infiltrating brines. As a result, this process could potentially increase the brine plume's volume and vertical or/and lateral extent beyond that which predictive models without vapor transport may indicate.

[3] In stratified soils, which are typical of natural sedimentary deposits, fine and coarse layers are interbedded. Lateral transport of infiltrating solutions is likely to occur at the fine over coarse interface, due to capillary barrier effects [*Kung*, 1990; *Selker*, 1998]. Lateral heterogeneity is ubiquitous in natural sedimentary deposits, as is the case at the Hanford site, and is likely to lead to predominantly lateral flow [*Selker et al.*, 2000; *Weisbrod et al.*, 2000b]. If brine is transported laterally along the interfaces between the fine and coarse layers, water vapor could potentially be drawn into the brine, increasing the extent of lateral transport of the brine.

[4] Under static conditions, the total water potential in the vadose zone is commonly defined as the sum of matric, osmotic, pressure, and gravitational energy components [*Hillel*, 1998]. In most natural systems, the pore water is relatively dilute and pressure and osmotic potentials are often neglected. Thus the total hydraulic head is often taken to be the sum of matric and gravitational potentials. However, for highly concentrated solutions, a clear distinction is necessary between the convective flux of the solution and the diffusive flux of the water vapor. For systems at or near gravitational equilibrium, i.e. static, the diffusive flux of water vapor may become the predominant mode of mass transport.

[5] In isothermal systems, water vapor flux is partly controlled by the osmotic potential, which can be determined from the solution chemistry data [*Corey and Klute*, 1985; *Hillel*, 1998]. It is worth noting that it is difficult physically to separate liquid from vapor movement com-

[1] Now at CH2M HILL, Corvallis, Oregon, USA.

0043-1397/03/2002WR001539

pletely, since the two are naturally linked in complex processes consisting of evaporation, vapor diffusion, condensation, short-range liquid flow, etc. [*Philip and de Vries*, 1957]. The relationship between salt concentration and osmotic potential is well documented in the literature [e.g., *Bresler et al.*, 1982; *Zemaities et al.*, 1986] and is not discussed in this manuscript.

[6] Vapor flux can be divided into thermal and isothermal flux. Vapor density is highly sensitive to changes in temperature, and therefore thermal vapor flux is generally considered much more important than isothermal vapor flux [*Scanlon et al.*, 1997, 2000]. Most efforts have been extended toward better understanding the mechanisms of thermal vapor transport in both experimental work and modeling [e.g., *Kneafsey and Pruess*, 1998; *Philip and de Vries*, 1957; *Pruess*, 1983, 1997; *Xu and Preuss*, 2001]. Isothermal vapor flux has often been neglected in the vadose zone except in the upper few meters where brines may develop due to aggressive evaporation under arid conditions [e.g., *Scanlon et al.*, 2000; *Weisbrod et al.*, 2000a].

[7] Isothermal vapor flux is driven by a gradient in vapor density. The vapor density, or water vapor pressure, P_v, at a solution interface can be calculated using the following equation:

$$P_v = \exp\left(\frac{-(\psi_s + \psi_\tau)\overline{V}_w}{RT}\right)P_v^0 \quad (1)$$

where P_v^0 is the saturated water vapor density at absolute temperature T, R is the gas constant (8.3143×10^{-6} m^3 Mpa/mole/K), $\overline{V}_w$ is the partial molal volume of water (18.0×10^{-6} m^3/mole), ψ_s is the matric potential, and ψ_τ is the osmotic potential (Mpa). The gradient in vapor density due to variation in matric potential under isothermal conditions is generally negligible. The relationship between salinity, osmotic potential and vapor density is given in Figure 1, for a $NaNO_3$ solution at 20°C.

[8] Gradients in osmotic potential can induce flow in either the liquid or gas phases. However, for liquid water to flow under such an osmotic gradient, a semi-permeable membrane is required. A semi-permeable membrane excludes aqueous ions, as seen across plant root cell walls. In soils, this occurs when anions are excluded from negatively charged soil pores which act as a semi-permeable membrane, and is most common in clays due to their charged surfaces [*Sposito*, 1989; *Kemper and Rollins*, 1966]. In the vapor phase, the gas-filled pores act as a membrane between the low-and high-concentration fluids.

[9] Water content and salt distribution in columns packed with uniformly wetted soils, in response to the emplacement of crystalline salt at one end, was studied by *Kelly and Selker* [2001], *Scotter* [1974], *Scotter and Raats* [1970], and *Wheeting* [1925]. The authors observed the accumulation of water near the salt crystals and explored the effect of soil texture, water content, and salt type. The combined effect of salt type, soil texture, and temperature on water movement was explored by *Nassar and Horton* [1989a, 1989b] and *Nassar et al.* [1992]. Theoretical analysis and modeling of water movement in the presence of osmotic gradients have been carried out by *Parlange* [1973], *Scotter* [1974], and *Kelly* [1998]. However, studies exploring water vapor transport between imbibing saline solutions and the surrounding matrix have not been published, to our knowledge.

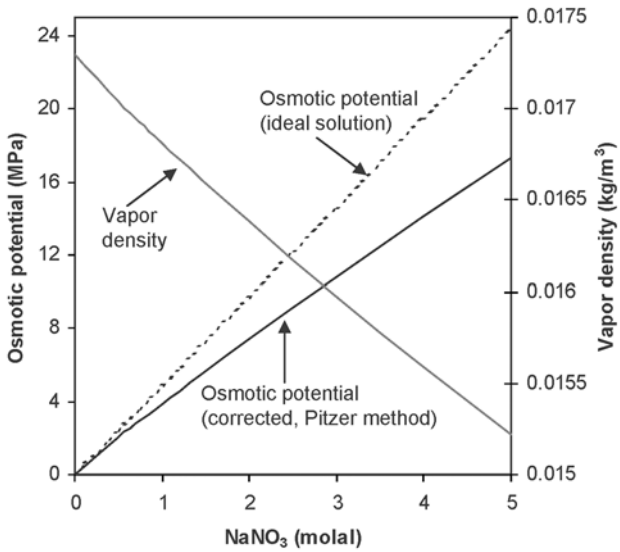

Figure 1. The effect of $NaNO_3$ concentration on (1) the osmotic potential for ideal solutions (low concentration), (2) the osmotic potential after incorporating the osmotic coefficient, and (3) the vapor density, all at 20°C. Note that these parameters vary for different salts and are sensitive to changes in temperature. Osmotic coefficient was calculated according to Pitzer's equation [*Zemaities et al.*, 1986].

[10] The objectives of this work were to study experimentally the transport of water vapor into imbibing brine in homogeneous and layered unsaturated sands. A series of laboratory experiments were carried out in 2-D chambers packed with translucent silica sand. Relative changes in light transmission were used to quantify saturation variations in the vicinity of $NaNO_3$ brines applied over time. Four sand grades were considered, both in homogeneous and layered systems. The potential impact of osmotically driven water vapor transport in natural settings, such as the Hanford site, was evaluated.

2. Materials and Methods

2.1. Experimental Setup

[11] The light transmission system consisted of a chamber, light source, and detector. The chamber, which contained the porous media, consisted of two glass panels separated by a U-shaped aluminum spacer mounted to a light source. A digital CCD camera was used to quantify light transmission. A more detailed description of this setup is provided by *Niemet and Selker* [2001] and *Weisbrod et al.* [2002]. Accusand (Unimin, Le Sueur, MN), silica sands in four different grades, was used as the porous media. Major physical and mineralogical properties of the sand are summarized by *Schroth et al.* [1996]. Five experiments were performed in homogenous packs of a single grade of 12/20, 20/30, 30/40, or 40/50 sand (experiments 1–5, Table 1), and two were performed in packs consisting of two fine sand layers (40/50) embedded in coarser (20/30) sand (experiments 6–7). The packing

Table 1. List of Experiments

Experiment	Sand Grade	Packing	Solution Applied			Sampled	ϕ	Remarks
			Left Plume	Center Plume	Right Plume			
1	12/20	homogenous	***A***	***C***	***B***	no	0.343	
2	20/30	homogenous	***A***	***C***	***B***	yes	0.334	
3	30/40	homogenous	***A***	***D***	***E***	no	0.336	
4	30/40	homogenous	***A***		***B***	yes	0.333	
5	40/50	homogenous	***A***	***C***	***B***	yes	0.339	prewetted with ***A***
6		layered		***C***		no	0.340	40/50 layers in 20/30
7		layered		***A***		yes	0.340	same pack as experiment 6

procedure for all the homogenous experiments was carried out with dry sand as described by *Niemet and Selker* [2001].

[12] The layered systems utilized two capillary wick cords (Amatex HD 3/8) placed against the inside of the aluminum spacer from the top of the manifold to the top of the glass. The wick cords maintained hydraulic continuity between the fine layers and the capillary fringe to facilitate drainage of the fine layers (Figure 2). The layered packs required five separate lifts during packing, where each layer was vacuumed flat after pouring. The sequence of layers included (bottom to top): 27 cm of 20/30 sand, 3.0 cm 40/50 sand, 15 cm of 20/30, 2 cm of 40/50, and 8 cm of 20/30 on top; all layers extended at the width of the chamber and touched the wick cords at both ends. The ratio of the d_{50} values between the 40/50 and 20/30 was 0.504.

[13] Five different solutions, designated ***A***–***E***, were used in the infiltration experiments and are identified in Table 2. Some physical properties of the solutions are given in Table 2. It is worth mentioning that the differences in surface tension, density, and viscosity between the solutions are important for imbibition, as will be discussed elsewhere, but are insignificant with regards to vapor transport.

2.2. Experimental Procedure

[14] Prior to each experiment the sand pack was initially saturated as described by *Weisbrod et al.* [2002]. The porosity (Table 1) of each pack was determined based on the volume of fluid required to saturate the sand, the mass of sand, and the volume of the chamber. Images were taken prior to and following saturation in all experiments, which were termed the "dry" and "saturated" images, as required for subsequent image processing. After saturation the chamber was allowed to drain slowly (<10 mL/min) for 24 hours, with the zero-pressure level held at the height of

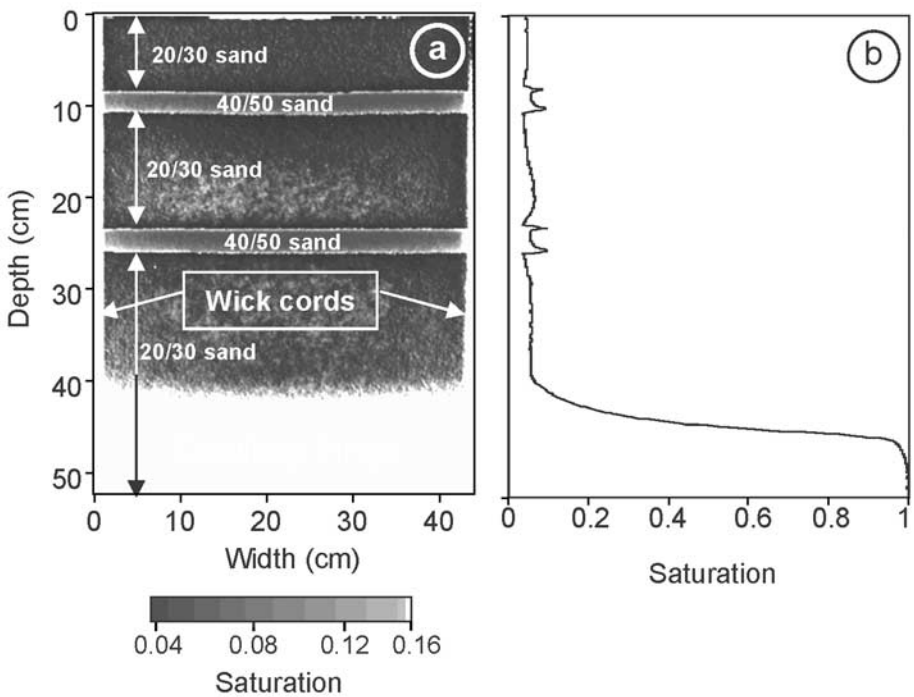

Figure 2. (a) A pseudo gray scale image of water saturation in the layered chamber, prior to the application of the solutions (experiments 6 and 7). The image was taken after the chamber was saturated and allowed to drain for 48 h, with zero pressure kept at the bottom of the chamber. (b) The average water saturation distribution as a function of depth.

Table 2. Solution Properties

Solution	Composition	Osmotic Potential, MPa	Osmotic Coefficent,[a]	Vapor Density, kg/m^3	Density, kg/m^3	Viscosity, cp	Surface Tension, mN/m
A	5 molal $NaNO_3$	17.3	0.71	0.0152	1247	1.314	80.54
B[b]	***A*** + 2% methanol	17.3	0.71	0.0152	1199	1.034	70.28
C	Pure water	0	1.0	0.0173	993	1.001	72.8
D	2 molal $NaNO_3$	7.4	0.76	0.0163	1095	1.117	75.19
E	0.75 molal $NaNO_3$	2.95	0.81	0.0169	1037	1.036	73.69

[a]Calculated by the Pitzer's method; see *Zemaities et al.* [1986] for more details.
[b]For the process described in this paper, solutions ***A*** and ***B*** can be considered identical.

the drainage manifold's upper surface. Following drainage the outflow pipe was closed. The vertical extent of saturated media near the bottom of the chamber (capillary fringe height) ranged from 7.5 to 23 cm, depending upon the grade of the sand used.

[15] In experiments 1–3 and 5, three evenly spaced 5 mL solution applications were dripped from syringe needles at a rate of 1 mL/min (Table 1). In experiment 4 two solutions were used. In the experiments carried out in the chamber packed with layered sand, one solution (either ***C*** or ***A***, experiments 6 and 7, respectively) was applied at the center. An image was taken immediately after injection, followed by 10 min imaging intervals for 3 h, 1 h intervals 3–24 h from injection, 2 h intervals 24–48 h from injection, and 3 h intervals 48–72 h from injection. In some of the experiments additional images were taken beyond 72 h.

[16] Following some of the experiments (Table 1), the chamber was dissembled and sand samples were taken from the chamber at selected locations. Each sample was weighed then oven dried at 55°C for 48 h to determine the water saturation. 5 g from each dry sample were mixed with 10 mL of double distilled water and shaken for 12 h. The electrical conductivity (EC) of the supernatant was measured (GLA® Instant EC Salinity Drop Tester) and the salinity of the soil solution was determined using a calibration curve between EC and $NaNO_3$ concentration.

[17] All image manipulations were performed on a pixel-by-pixel basis using Transform 3.4 (Fortner Software LLC). Water saturation was determined from the light transmission images as described by *Niemet et al.* [2002]. Images depicting the resulting changes in saturation, ΔS, were developed using a 16-band gray scale palette showing negative changes in saturation from 0 to $-S_{res}$. The palette proceeds from white (least change) to black (greatest change). In the layered experiments (experiments 6–7) it was necessary to determine saturation separately depending on the media type at a given pixel. In this case, the drying effect above and below the fine layer was more clearly distinguished in terms of saturation (S) rather than the change in saturation (ΔS) as used for the homogeneous experiments (Figure 2). It should be noted that high concentrations of salts increase the index of refraction of the liquid and consequently affect the saturation values measured using the light transmission method. The magnitude of this effect for a given salt depends on the combination of salt concentration and the degree of liquid saturation and therefore is difficult to correct for accurately. While this complication does slightly affect saturation values within the saline solution, and would be of concern if precise mass balance were required, it does not influence the saturation values determined outside of the saline plumes, which is the primary area of interest in this paper.

3. Results

[18] The results described in this paper focus on the transport of water vapor into the saline plumes from the surrounding native media. The temperature-dependent component of vapor flux was not considered, as it was assumed that isothermal conditions existed within the chamber. The transport mechanisms of the imbibing liquids in relation to their fluid properties will be discussed elsewhere.

[19] Since the primary areas of interest within the chamber were at or near residual saturation prior to the addition of the plumes, and their saturation decreased due to the vapor extraction drying, the maximum observable range in saturation is equal to the residual saturation for each of the respective sand grades (3–5%). Furthermore, drying below residual involves the disintegration of the thin films of water coating the sand grains, which when in place are significantly more conductive to light transmission than the uncoated surfaces. Hence a small change in saturation produces a disproportionally large change in transmitted light.

3.1. Homogenous Media

[20] Similar phenomena were observed in all sand grades, therefore only one example is shown where two, similar, hypersaline solutions (***A*** and ***B***) were applied to 30/40 sand grade (experiment 4, Figure 3). In all sand grades, the lateral extent of the drying zones around the infiltrating brine, where water saturation was reduced to below residual, increased over time. Lateral cross sections at 10-cm-depth at different times are shown in Figure 3b. $NaNO_3$ concentrations at the plume's center-line (***A*** and ***B***) were similar throughout the top 15 cm (~1.2–2 M). Below 15 cm the salt concentration within ***B*** became higher than within ***A*** (>2.5 M versus ~1.5 M). Note that gravimetric salt concentration measurements were taken at the end of the experiment (~132 h from application).

[21] If a fresh water plume is applied into sand prewetted with brine, vapor from the pure water plume is expected to diffuse out into the surrounding saline environment. In experiment 5, 40/50 sand was prewetted with solution ***A*** rather than ***C***, and solutions ***A***, ***B***, and ***C*** were applied. As expected, following the direction of the osmotic gradient, solution ***C*** migrated out of the plume into the residual brine. Eventually, the water saturation within the initial area of plume ***C*** was reduced until almost dry (Figure 4a). At the end of the experiment (~90 h from application), the $NaNO_3$

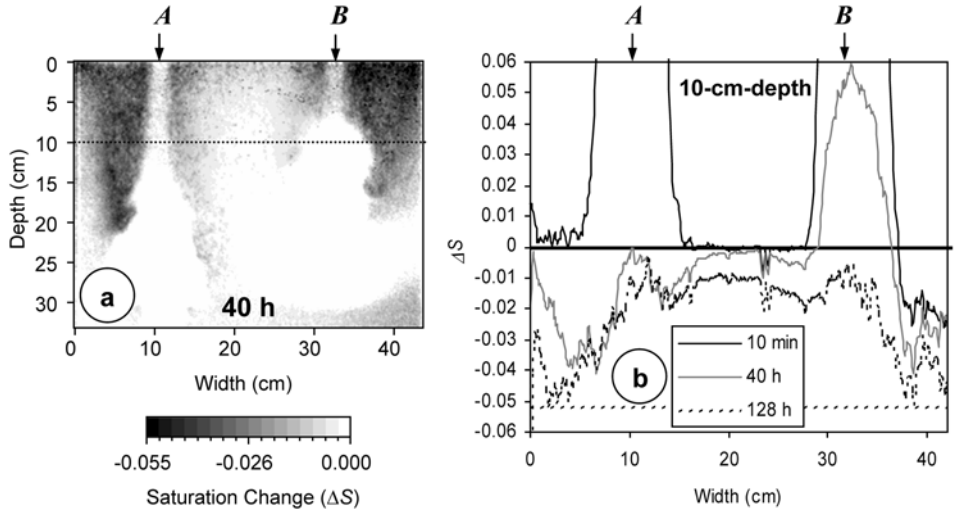

Figure 3. (a) Experiment 4 (40 h from application) where solutions ***A*** and ***B*** were applied to 30/40 sand prewetted with pure water ***C***. The pseudo gray scale image shows the negative changes in saturation (ΔS) with respect to before the solutions were applied. (b) Three cross sections at 10 cm depth 10 min, 40 h, and 128 h from application.

concentration was ~1.6 M at the centerline of plume ***C*** area and ~5 M all around it. Lateral cross sections 10 min, 5 h, and 40 h from application, at 10 cm depth are shown in Figure 4b.

3.2. Heterogeneous Media (Layered System)

[22] Before the solutions were applied, the saturation in the fine layers was 5–6%, where as in the surrounding coarse sand it was 3–4% (Figure 2). When solutions ***C*** and ***A*** were applied (experiments 6 and 7, respectively), they migrated downward until penetrating the uppermost fine layer, at which point they spread within the fine layer due to the combination of increased capillarity and a capillary barrier at the interface of the fine with the underlying coarse sand layer. In experiment 6, where fresh water, ***C***, was applied, the water moved laterally until reaching equilibrium. On the other hand, when solution ***A*** was applied (experiment 7), drying was observed at the boundaries of the migrating brine both along the vertical and the horizontal brine-fresh water interface. Figure 5 shows the saturation distribution 24 h from application of solutions ***C*** and ***A***. Additionally, a partial vertical cross section through the upper fine layer, at 30 cm width, shows the areas influenced by the vapor extraction above and below the layer when

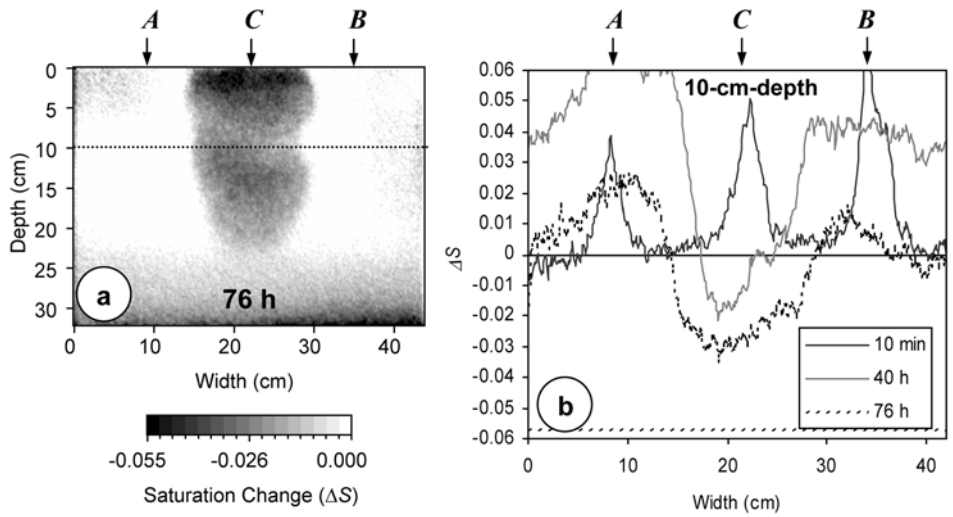

Figure 4. (a) Experiment 5 (76 h from application) where solutions ***A***, ***C***, and ***B*** were applied to 40/50 sand prewetted with solution ***A***. The pseudo gray scale image shows the negative changes in saturation (ΔS) with respect to before the solutions were applied. (b) Three cross sections at 10 cm depth 10 min, 40 h, and 76 h from application. Note the $\Delta S < 0$ values zones developed over time within the area where ***C*** was applied.

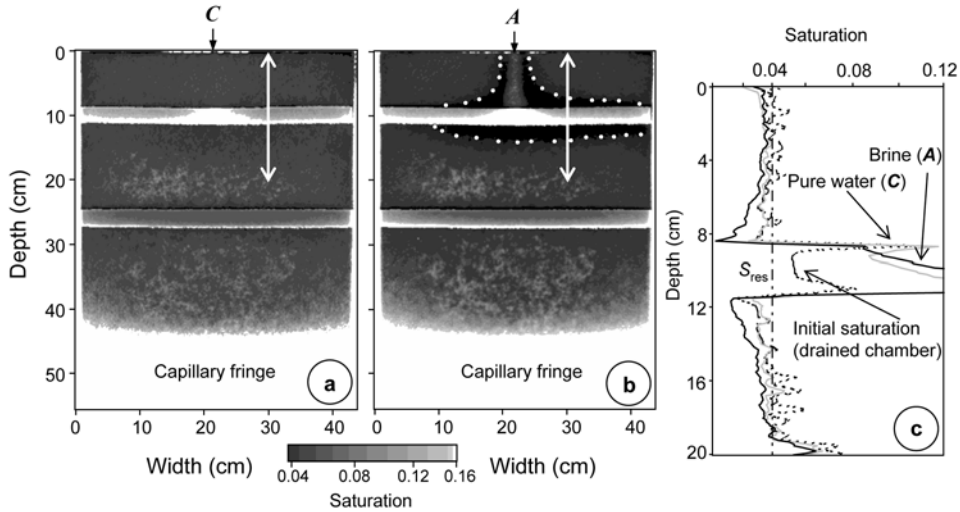

Figure 5. Pseudo gray scale images of water saturation in the layered chamber (experiments 6 and 7), 24 h from application of solutions ***C*** (a) and ***A*** (b). (c) Partial vertical cross sections of water saturation at the upper 20 cm (see arrows in Figures 5a and 5b), 24 h from application. Note the $S < S_{res}$ zones at the fine/coarse interface where the brine (***A***) migrated laterally. For clarification, these areas are indicated with white dots (Figure 5b).

solution ***A*** was applied (Figures 5b and 5c). As in the homogenous pack, the extent of the dry areas increased over time.

4. Discussion

[23] The drying patterns observed in all experiments were generally consistent with the vapor stripping patterns seen by *Scotter and Raats* [1970] and *Kelly and Selker* [2001]. The consistency with the results of those previous studies is somewhat surprising for a number of reasons. First, the moisture content was not constant both in and around the infiltrating plumes. Second, the salt concentration was variable in space and time within each plume. Third, the downward wetting front velocity was different between sand grades and between solutions in the same sand grade. Finally, the shapes of the plumes varied over time, changing the location of the brine-fresh water interface throughout the experiments. Apparently, although preventing accurate quantitative calculations, these variations were not sufficient to alter fundamentally the structure of the diffusion-based process.

[24] Destructive sampling at the end of the experiments showed that concentrations at the centerlines of the saline plumes varied between 1 and 2.3 M. While only 5 mL of brines were applied to the chamber in our experiments, in natural settings large volumes of saline solutions may leak from tanks, pipes, evaporation ponds, etc. into the native soil. This, in turn, could provide a continual source of fresh water that could be delivered into the contaminant plume via water vapor transport. Neglecting the natural heterogeneity of the subsurface, changes in water content, and recharge, it appears reasonable to assume that vapor-stripping behavior would scale with the square root of time over long periods [*Parlange*, 1973]. Our experiments showed roughly, that the saline plume desiccated 1.5 cm from the surrounding fresh water after 1 day, and about 3 cm after 4 days. Following this trend, taking net percolation to be negligible, and under constant maximum gradient, after ~2700 y up to 15 m around a percolating brine plume would be stripped of resident water. Water vapor extraction may occur either along the infiltrating plumes in homogenous media or above and below if the plume transported laterally within a thin fine layer. Vapor stripping estimation is probably an upper boundary because the brine transport will end up equilibrating the vapor density between the plume and the surrounding pure water.

[25] A calculation, based on an error function solution of the diffusion equation [*Crank*, 1975], and using Penman's formulation of the saturation-dependent gas diffusion coefficient [*Penman*, 1940] reveals that a maximum of ~6 m^3 of water vapor would be extracted per square meter of brine/fresh water interface (assuming constant concentra-

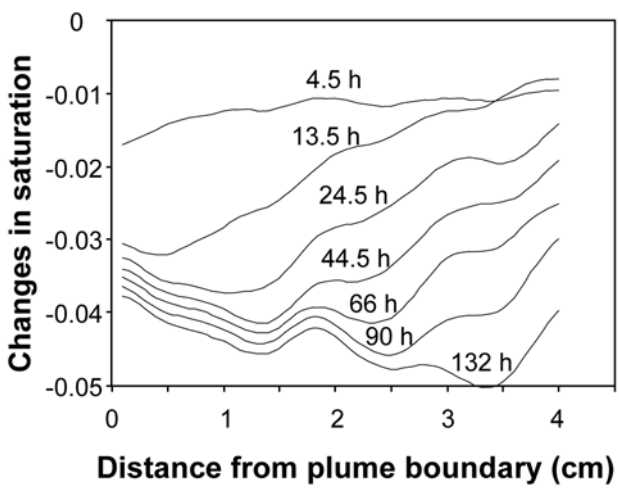

Figure 6. Lateral saturation cross sections at seven different times. The cross sections were taken to the left boundary of plume ***A*** in experiment 4.

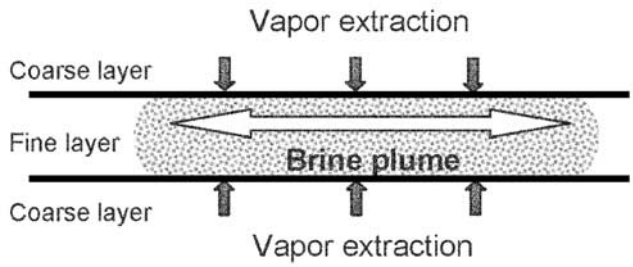

Figure 7. Mechanistic illustration of the lateral migration of hypersaline contaminant plume in layered sediments where the capillary barrier effect takes place. The water vapor transport into the plume increases the pollutant volume while slightly diluting the migrating plume.

tion of 5 M within the plume and fresh water out of the plume) via vapor extraction after 10,000 days (~27 years). However, in reality, dilution of the brine will reduce vapor extraction over time and recharge is likely to change water distribution. On the other hand, the size of the plume will grow over time, increasing the overall surface area for extraction. This process is limited mainly by the final dilution of the brine to a concentration sufficiently low to cease vapor transport. According the results of *Kelly et al.* [1997], the minimum concentration needed to activate the vapor stripping is in order of 0.05 M, roughly 100 times lower than the initial $NaNO_3$ concentration used in our experiments and the solutions leaked from the Hanford tanks.

[26] The long-term behavior of the vapor stripping phenomena can be observed in Figure 6. Five cross sections from the left side of plume ***A*** (experiment 4, Table 1) are shown. The zero position was set to be the left edge of the brine after 4.5 h at 10 cm depth. Generally, drying increases in magnitude and extends outward laterally from the brine plume over time. The temporal drying phenomenon is likely controlled by the coupled contributions of the spatially variable saturation, and vapor transport. Although appropriate numerical modeling of this situation was beyond the scope of this work, a more rigorous quantitative analysis is warranted in future research.

[27] As noted before, stratified sedimentary materials are common in nature and dominate the geologic character of the Hanford formation, where horizontal movement may be prevalent over vertical infiltration due to capillary barrier effects. A current estimation for the lateral contaminant expansion during emplacement is in the order of ~20 m [*Pruess et al.*, 2000]. Stripping vapors from the native soils above and below these fine layers, as shown in Figure 5, may substantially enhance the lateral movement of these contaminant plumes as shown in Figure 7. If the horizontal layer is penetrated by natural fractures, macropores, observation wells, or terminate at the surface, the contaminants may unexpectedly reach either the deep vadose zone and/or the water table or seep slowly to the land surface.

5. Summary and Conclusions

[28] Water vapor transport from residually saturated native sand into imbibing brines was demonstrated in a series of laboratory experiments carried out in 2-D light transmission chambers. Differences in osmotic potential between the infiltrating and resident fluids, and consequently the vapor density gradient, induce diffusive water vapor flux into the brine. The empty pores at low saturation act as a conduit and semi permeable membrane between the brine and fresh water, through which water vapor can pass. Water vapor is stripped from the surrounding native media regardless of whether the brine migrates vertically downward or laterally due to the existence of a capillary barrier. Transitions between fine and coarse layers in the subsurface, leading to lateral transport through the fine layer, are common in natural settings such as the Hanford formation. Therefore enhanced lateral migration of contaminants due to water vapor extraction is of special interest.

[29] An order-of-magnitude calculation (ignoring the coupled flow of liquid brine from the plume toward the surrounding environment) suggests that over long periods of time a significant amount of water can delivered from the native sediments into a brine plume by vapor transport. This process is limited mainly by the vapor diffusion rate and the dilution of the imbibing brine. The water vapor, once incorporated into the saline plume, may enhance the transport of contaminants in the subsurface. Our results suggest that the transport of water vapor should be considered in predictive models where the migration of hypersaline solutions is considered. Further research is required to investigate the impact of the variable boundary conditions before more quantitative predictions can be made.

[30] **Acknowledgments.** We would like to thank two anonymous reviewers for their thorough and constructive review, which significantly improved this manuscript. This work was funded by the Department of Energy under contract number DE-FG07-98ER14925.

References

Bresler, E., B. L. McNeal, and D. L. Carter, *Saline and Sodic Soils*, Springer-Verlag, New York, 1982.

Corey, A. T., and A. Klute, Application of the potential concept to soil water equilibrium and transport, *Soil Sci. Soc. Am. Proc.*, *30*, 529–534, 1985.

Crank, J., *The Mathematics of Diffusion*, 2nd ed. Oxford Univ. Press, New York, 1975.

Grand Junction Projects Office, Vadose zone characterization project at the Hanford Tank Farms, SX Tank farm report, *GJ-HAN-DOE/ID12548-268(GJPO-HAN-4)*, U.S. Dep. of Energy, Grand Junction, Colo., 1996.

Hillel, D., *Environmental Soil Physics*, Academic, San Diego, Calif., 1998.

Kemper, W. D., and J. B. Rollins, Osmotic efficiency coefficients across compacted clays, *Soil Sci. Soc. Am. J.*, *49*, 3–11, 1966.

Kelly, S. F., Non-convective ion movement in unsaturated porous media, Ph.D. dissertation, Oreg. State Univ., Corvallis, 1998.

Kelly, S. F., and J. S. Selker, Osmotically driven water vapor transport in unsaturated soils, *Soil Sci. Soc. Am. J.*, *65*, 1634–1641, 2001.

Kelly, S. F., J. L. Green, and J. S. Selker, Fertilizer ion movement in a protected diffusion zone, *J. Am. Soc. Hort. Sci.*, *122*, 122–128, 1997.

Kneafsey, T. J., and K. Pruess, Laboratory experiments on heat-driven two-phase flows in natural and artificial rock features, *Water Resour. Res.*, *34*, 3349–3367, 1998.

Kung, K.-J. S., Preferential flow in a sandy vadose soil, 2. Mechanism and implications, *Geoderma*, *46*, 59–71, 1990.

Nassar, I. N., and R. Horton, Water transport in unsaturated nonisothermal salty soil: I. Experimental results, *Soil Sci. Soc. Am. J.*, *53*, 1323–1329, 1989a.

Nassar, I. N., and R. Horton, Water transport in unsaturated nonisothermal salty soil: II. Theoretical development, *Soil Sci. Soc. Am. J.*, *53*, 1330–1337, 1989b.

Nassar, I. N., R. Horton, and A. M. Globus, Simultaneous transfer of heat, water and solute in porous media: II. Experiment and analyses, *Soil Sci. Soc. Am. J.*, *56*, 1357–1365, 1992.

Niemet, M. R., and J. S. Selker, A new method for quantification of liquid saturation in 2D translucent porous media systems using light transmission, *Adv. Water Resour.*, *24*, 651–666, 2001.

Niemet, M. R., M. L. Rockhold, N. Weisbrod, and J. S. Selker, Relationships between gas-liquid interfacial surface area, liquid saturation and light transmission in variably saturated porous media, *Water Resour. Res.*, *38*(8), 1135, doi:10.1029/2001WR000785, 2002.

Parlange, Y.-J., Movement of salt and water in relatively dry soils, *Soil Sci.*, *116*, 249–255, 1973.

Penman, H. L., Gas and vapor movements in the soil: 1. The diffusion of vapors through porous solids, *J. Agric. Sci.*, *30*, 437–461, 1940.

Philip, J. R., and D. A. de Vries, Moisture movement in porous materials under temperature gradients, *Eos Trans. AGU*, *38*, 222–232, 1957.

Pruess, K., Heat transfer in fractured geothermal reservoirs with boiling, *Water Resour. Res.*, *19*, 201–208, 1983.

Pruess, K., On vaporizing water flow in hot sub-vertical rock fractures, *Transp. Porous Media*, *28*, 335–372, 1997.

Pruess, K., P. C. Lichter, C. I. Steefle, M. D. White, and S. B. Yabusaki, Simulation studies of unsaturated flow at Hanford Tanks, *Eos Trans. AGU*, *81*(48), Fall Meet. Suppl., abstract H52D-05, 2000.

Scanlon, B. R., S. W. Tyler, and P. J. Wierenga, Hydrologic issues in arid, unsaturated systems and implication for contaminant transport, *Rev. Geophys.*, *35*, 461–490, 1997.

Scanlon, B. R., J. P. Nicot, and J. M. Massmann, Soil gas movement in unsaturated systems, in *Handbook of Soil Science*, edited by M. E. Sumner, pp. A-277–A-319, CRC, Boca-Raton, Fla., 2000.

Schroth, M. H., S. J. Ahern, J. S. Selker, and J. D. Istok, Characterization of Miller-similar silica sands for laboratory hydrologic studies, *Soil Sci. Soc. Am. J.*, *60*, 1331–1339, 1996.

Scotter, D. R., Factors influencing salt and water movement near crystalline salts in relatively dry soil, *Aust. J. Soil Res.*, *12*, 77–86, 1974.

Scotter, D. R., and P. A. C. Raats, Movement of salt and water near crystalline salt in relatively dry soil, *Soil Sci.*, *109*, 170–178, 1970.

Selker, J. S., Design of interface shape for protective capillary barriers, *Water Resour. Res.*, *33*, 259–260, 1998.

Selker, J. S., A. Ward, M. R. Niemet, N. Weisbrod, and C. Cooper, Field observations of transport of high concentration solutions in unsaturated sedimentary materials, *Eos Trans. AGU*, *81*(48), Fall Meet. Suppl., abstract H61A-01, 2000.

Sposito, G., *The Chemistry of Soils*, Oxford Univ. Press, New York,, 1989.

Weisbrod, N., R. Nativ, A. E. Adar, and D. Ronen, Salt accumulation and flushing in unsaturated fractures in an arid environment, *Ground Water*, *38*, 452–461, 2000a.

Weisbrod, N., J. S. Selker, M. R. Niemet, T. McGinnis, C. Cooper, and A. Ward, Transport mechanisms of highly concentrated solutions in layered unsaturated sedimentary basin, paper presented at Annual Meeting, Geol. Soc. of Am., Reno, Nev., 2000b.

Weisbrod, N., R. M. Niemet, and J. S. Selker, Imbibition of saline solutions into dry and prewetted porous media, *Adv. Water Resour.*, *25*(7), 841–855, 2002.

Wheeting, L., Certain relationships between added salts and the moisture of soils, *Soil Sci.*, *16*, 287–299, 1925.

Xu, T., and K. Preuss, Modeling multiphase non-isothermal fluid flow and reactive geochemical transport in variably saturated fractured rocks: 1. Methodology, *Am. J. Sci.*, *301*, 16–33, 2001.

Zemaities, J. F., D. M. Clark, M. Rafal, and N. C. Scrivner, *Handbook of Aqueous Electrolyte Thermodynamics*, Am. Inst. of Chem. Eng., New York, 1986.

T. McGinnis and J. S. Selker, Department of Bioengineering, Oregon State University, Corvallis, OR 97331, USA.

M. R. Niemet, CH2M HILL, Corvallis, OR 97330, USA.

N. Weisbrod, Department of Environmental Hydrology and Microbiology, Institute for Water Sciences and Technologies, Desert Research Institutes, Ben-Gurion University of the Negev, Sede-Boqer Campus 84990, Israel. (weisbrod@bgumail.bgu.ac.il)